

1 Calcification in a marginal sea – influence of seawater $[Ca^{2+}]$ and carbonate chemistry on
2 bivalve shell formation

3
4 Jörn Thomsen¹, Kirti Ramesh^{1,2}, Trystan Sanders¹, Markus Bleich², Frank Melzner¹
5 ¹Marine Ecology, GEOMAR Helmholtz Centre for Ocean Research, Kiel, Germany
6 ²Institute of Physiology, Christian-Albrechts-University Kiel, 24098 Kiel, Germany

7
8 Running headline: Abiotic effects on mussel calcification

9
10 **Abstract**

11 In estuarine coastal systems such as the Baltic Sea, mussels suffer from low salinity which
12 limits their distribution. Anthropogenic climate change is expected to cause further
13 desalination which will lead to local extinctions of mussels in the low saline areas. It is
14 commonly accepted that mussel distribution is limited by osmotic stress. However, along the
15 salinity gradient environmental conditions for biomineralization are successively becoming
16 more adverse as a result of reduced $[Ca^{2+}]$ and dissolved inorganic carbon (C_T) availability.
17 In larvae, calcification is an essential process starting during early development with
18 formation of the prodossoconch I (PD I) shell which is completed under optimal conditions
19 within 2 days.

20 Experimental manipulations of seawater $[Ca^{2+}]$ start to impair PD I formation in *Mytilus* larvae
21 at concentrations below 3 mM, which corresponds to conditions present in the Baltic at
22 salinities below 8 g kg⁻¹. In addition, lowering dissolved inorganic carbon to critical
23 concentrations (<1 mM) similarly affected PD I size which was well correlated with calculated
24 $\Omega_{\text{Aragonite}}$ and $[Ca^{2+}][HCO_3^-]/[H^+]$ in all treatments. Comparing results for larvae from the
25 western Baltic with a population from the central Baltic revealed significantly higher tolerance
26 of PD I formation to lowered $[Ca^{2+}]$ and $[Ca^{2+}][HCO_3^-]/[H^+]$ in the low saline adapted
27 population. This may result from genetic adaptation to the more adverse environmental
28 conditions prevailing in the low saline areas of the Baltic.

29 The combined effects of lowered $[Ca^{2+}]$ and adverse carbonate chemistry represent major
30 limiting factors for bivalve calcification and can thereby contribute to distribution limits of
31 mussels in the Baltic Sea.

32
33 **Key-words**

34 Baltic Sea, bivalves, calcium, calcification, carbonate chemistry, climate change

35
36 **1. Introduction**

37 Salinity is one of the most important environmental parameters limiting the distribution of
38 aquatic species. Many marine organisms exhibit little tolerance to reduced salinity and are
39 thus not able to thrive in brackish water environments influenced by riverine inputs (Whitfield
40 et al. 2012). On the other hand, some animals, such as bivalves and crustaceans tolerate the
41 dilution of the ambient seawater and are able to inhabit estuarine, brackish water habitats
42 (Westerbom et al. 2002). However, within these habitats, organisms need to tolerate a
43 number of environmental stressors which are changing concomitantly.

44 Generally, lowered ambient ion concentrations affect an organism's ability to maintain
45 cellular homeostasis. In response, some organisms such as crustaceans actively regulate
46 the ionic composition of their extracellular fluids. However, mytilid mussels do not control
47 haemolymph osmolarity and ionic composition mostly corresponds to that of ambient
48 seawater (Thomsen et al. 2010). Thus tissues are subjected to a diluted medium in brackish
49 water but the inorganic composition of the intracellular space needs to be regulated in order
50 to maintain enzymatic functions. At moderately lowered salinity, intracellular $[K^+]$ and $[Na^+]$
51 are kept relatively stable at about 200 and 100 mM, respectively, but $[K^+]$ drops rapidly under
52 strong hypoosmotic stress to avoid cell swelling (Willmer 1978, Wright et al. 1989; Silva and
53 Wright 1994). In order to stay iso-osmotic with their environment following long-term
54 acclimation to lowered salinity, intracellular $[K^+]$ and $[Na^+]$ are maintained at lower
55 concentrations (Willmer 1978, Natochin et al. 1979). In addition, bivalves reduce the

56 concentration of intracellular compatible organic osmolytes (Hochachka and Somero 2002)
57 such as certain amino acids, taurine and betaine during the acclimation phase (Silva and
58 Wright 1994, Kube et al. 2006). However, at a certain critical salinity threshold (S_{crit}), the
59 intracellular organic osmolyte pools are depleted which has been suggested to eventually
60 limit species fitness (Kube et al. 2006; Podbielski et al. 2016).

61 At the same time, bivalves produce an external shell composed of $CaCO_3$ and an organic
62 matrix (Falini et al. 1996). The shell enables adult bivalves to live in intertidal habitats and is
63 an effective protection against predation but shell formation has been shown to be sensitive
64 to lowered salinity (Malone and Dodd 1967). Under favourable environmental conditions,
65 calcification begins already in early development and the first larval shell (prodissoconch I,
66 PD I) is completed within the first 48 hours after fertilization. PD I formation is an important
67 prerequisite for the successful development of bivalve larvae as larvae seem to commence
68 feeding only after completion of the shell which provides structural support (e.g. muscle
69 attachment site) for the functional velum (Lucas and Rangel 1983; Cragg 1985). However,
70 PD I formation is highly sensitive to chemical and environmental stressors (Williams and Hall
71 1999) and initiation of feeding is delayed under adverse carbonate chemistry (Waldbusser et
72 al. 2015).

73 Recently, a number of studies investigated how changes of seawater carbonate chemistry
74 affect marine calcifiers. Those studies were mostly motivated by the ongoing input of
75 anthropogenic CO_2 into the oceans which results in a drop of pH and lowered $[CO_3^{2-}]$, a
76 process called ocean acidification. Bivalve shell formation is highly sensitive to modifications
77 of carbonate chemistry and therefore negatively affected by ocean acidification (Gazeau et al.
78 2013; Waldbusser et al. 2014; Thomsen et al. 2015). The exact reason for the sensitivity of
79 calcification to adverse carbonate chemistry is still under debate (Cyronak et al. 2015).
80 Lowered saturation of seawater with respect to calcium carbonate (Ω , $[Ca^{2+}][CO_3^{2-}]/K^*_{sp}$)
81 (with K^*_{sp} =stoichiometric solubility product (Mucci 1983)) could affect the kinetic of shell
82 formation (according to $r = k(\Omega-1)^n$ with r =mineral precipitation rate, k =rate constant and
83 n =reaction order, Waldbusser et al. 2014) and undersaturation leads to dissolution of existing
84 calcium carbonate structures (Thomsen et al. 2010; Melzner et al. 2011, Haynert et al. 2014).
85 Alternatively, the substrate inhibitor ratio (SIR) defined as the availability of the substrate for
86 calcification in the form of dissolved inorganic carbon (C_T) or HCO_3^- and the inhibitory effect
87 of lowered seawater pH (increased $[H^+]$) could restrict calcification rate (Bach 2015; Thomsen
88 et al. 2015; Fassbender, et al. 2016).

89 Independent of the exact mode of action, larval bivalve calcification is driven by uptake of
90 seawater Ca^{2+} and inorganic carbon (C_T) whereas metabolic carbon is only of minor
91 importance and contributes by less than 10 % in larvae and adults (McConnaughey and
92 Gillikin 2008, Waldbusser et al. 2015). Oceanic $[Ca^{2+}]$ is about 10 mM, but necessarily
93 linearly related with seawater salinity and thus reduced in estuaries. Freshwater $[Ca^{2+}]$ are in
94 general much lower (<1-2 mM $[Ca^{2+}]$, Ohlson and Anderson 1990; Juhna and Klavins 2000).
95 Oceanic C_T is about 2 mM whereby HCO_3^- and CO_3^{2-} contribute about 90 and 8 % to the C_T
96 pool, respectively. C_T of seawater equilibrated with the atmosphere is directly proportional to
97 salinity as it is depending on seawater total alkalinity (A_T). Therefore, calcifiers are facing
98 abiotic conditions in brackish water habitats which most likely affect their ability to form a
99 shell.

100 The Baltic Sea is an example of a brackish water habitat which is substantially influenced by
101 precipitation and riverine input (Gustafsson et al. 2014) which results in a salinity gradient
102 from 25 g kg^{-1} in the Kattegat transition zone to basically freshwater in the Gulfs of Riga,
103 Finland and Bothnia. As a consequence, $[Ca^{2+}]$, A_T and C_T decline linearly along the salinity
104 gradient (Kremling and Wilhelm 1997; Beldowski et al. 2010). However, varying composition
105 of riverine freshwater results in differing A_T -salinity correlations and in the Gulf of Riga, A_T
106 and thus C_T even increases with lowered salinity (Beldowski et al. 2010).

107 The Baltic Sea is among the coastal ecosystems which are most heavily influenced by
108 anthropogenic activity. Eutrophication enhanced hypoxia or even anoxia events in the
109 benthic ecosystem. As respiratory oxygen consumption is coupled to CO_2 production,
110 hypoxia is always accompanied by a pronounced increase of pCO_2 and thus affects the

111 carbonate system simultaneously (Melzner et al. 2013). Furthermore, climate change is
112 expected to increase precipitation in the Baltic catchment area which may cause increased
113 riverine runoff leading to reduced salinity (0 - 45 % reduction) in particular in the north-
114 eastern and central Baltic Sea (Meier et al. 2006; Gräwe et al. 2013). This shift in salinity will
115 most likely induce a substantial retreat of the marine fauna and flora and expansion of limnic
116 species into the formerly brackish water habitats (Johannesson et al. 2011).
117 Mytilid mussels (*Mytilus* spp.) are among the most abundant organisms of the Baltic Sea
118 (10^{13} individuals) contributing up to 90% to local hard bottom biomass, and thus are
119 important habitat builders (Enderlein and Wahl 2004, Johannesson et al. 2011). Their
120 distribution along the Finnish, Swedish and Estonian coast is limited by salinities of about 4.5
121 g kg^{-1} when abundance, biomass and growth drastically decline (Westerbom et al. 2002;
122 Martin et al. 2013; Riisgard et al. 2014). As growth combines both somatic growth and shell
123 formation, it is unclear which physiological mechanism exactly limits performance and
124 therefore the distribution of mussels (Riisgard et al. 2014).
125 Currently, distribution limits of marine bivalves in estuaries are commonly related to the
126 inability of intracellular osmoregulatory adjustment at lowered salinity (Maar et al. 2015).
127 However, as $[\text{Ca}^{2+}]$ and C_T availability decline along the Baltic Sea salinity gradient it is likely
128 that the calcification process is negatively affected as well. This process has not been
129 previously considered as a factor contributing to distribution limits of mussels. In this study,
130 we investigated the effects of seawater $[\text{Ca}^{2+}]$ independently of salinity in combination with
131 lowered C_T availability on the calcification performance of larval *Mytilus* spp. and correlated
132 the experimental data with environmental conditions present in the Baltic Sea.

134 2. Material and Methods

135 2.1 Animal collection and spawning

136 Adult mussels were collected from subtidal depths at the pier of GEOMAR in Kiel Fjord (shell
137 length: 4-6 cm, 54°19.8'N; 010°09.0'E) and at the wooden groynes close to Koserow on the
138 island of Usedom (shell length: 2-3 cm, 54°03.4'N; 014°00.4'E) between May and June 2016
139 (Fig. 1). Median salinity for Kiel Fjord and Usedom, located ~350 km east of Kiel, are ~ 17
140 and 7 g kg^{-1} , respectively (Table 1).

141 Mussels in the Baltic Sea represent hybrids of *Mytilus edulis* x *trossulus* with increasing
142 *trossulus* allele frequency towards the less saline, eastern Baltic (Stuckas et al. 2009). Thus
143 mussels collected in Kiel represent the Baltic *M. edulis*-like and animals from Usedom belong
144 to the *M. trossulus*-like genotype (Stuckas et al. 2017).

145 Specimens were either used for spawning immediately after collection or kept in cold storage
146 (9°C) in order to delay gonad maturation for up to 3 months. Stored mussels (ca. 500 g
147 mussel wet biomass per 20 L tank, 12 tanks) were fed 6 times a week with 500 mL of
148 *Rhodomonas* solution (ca. 2×10^6 cells mL^{-1}) supplemented with a commercial bivalve diet
149 (Acuinuga, Spain) and water was exchanged twice a week (Thomsen et al. 2010).
150 *Rhodomonas* spp. were cultured in PES medium as described previously with the exception
151 of using 40 L cylinders (Thomsen et al. 2010).

152 All experiments were performed at 17°C. Spawning was induced by exposing the animals to
153 rapidly elevated water temperature between 18-25°C using heaters. Spawning specimens
154 were separated from the remaining animals and eggs and sperms were collected individually
155 in beakers filled with 0.2 μm filtered seawater (FSW). Subsequently, eggs were pooled and
156 fertilized with a pooled sperm solution. For the Kiel population, 5 individual experimental runs
157 were performed with varying number of dams and sires used for crossings in each run. In
158 total 16 dams and 18 sires were used. For the Usedom population one run with 4 replicates
159 was performed for which gonads from 5 dams and 4 sires were pooled. Fertilization success
160 was determined by verifying the presence of a polar body and first and second cell division of
161 zygotes and was above 90% in all runs. Embryos (4-8 cell stage) and non-calcified
162 trochophora (in one experimental run of the Kiel population) from all parents were transferred
163 in equal numbers into the experimental units (volume: 25 or 50 mL in round plastic beakers)
164 at a density of 10 embryos/larvae mL^{-1} .

165 Three days post fertilization animals were removed from the experimental units by filtering
166 the full water volume through a filter with a mesh size of 20 μm or by collecting larvae
167 individually using a pipette in treatments with low survival. Subsequently, larvae were fixed
168 using 40 % paraformaldehyde (PFA, pH 8.0) resulting in a final PFA concentration of 4%.
169 Pictures of larvae were taken using a stereomicroscope (Leica M165 FC) equipped with a
170 Leica DFC 310 FX camera and LAS V4.2 software. Calcification was assessed by measuring
171 the larval shell length. PD I shell length was assessed using Image J 1.50i by measuring the
172 maximal shell length in parallel to the hinge or the maximal shell diameter for larvae that had
173 not developed a complete PD I shell.

174
175

176 2.2 Experimental manipulation of seawater $[\text{Ca}^{2+}]$ and carbonate chemistry

177 Artificial seawater (ASW) was prepared according to Kester (1967) for salinities of 14 and 7 g
178 kg^{-1} for experiments with *M. edulis*-like and *trossulus*-like, respectively, by adding NaCl,
179 NaSO_4 , KCl, NaHCO_3 , KBr, H_3BO_3 , MgCl_2 , CaCl_2 , and SrCl_2 to deionised water. Ca^{2+} free
180 artificial seawater (CFSW) was prepared by omitting CaCl_2 and adjusting osmolarity similar to
181 ASW by increasing NaCl concentrations. pH_{NBS} was adjusted to 8.0 using NaOH. All
182 experimental treatments comprised 5 % of 0.2 μm filtered seawater (FSW) from Kiel Fjord
183 which was adjusted to salinity 7 g kg^{-1} for the Usedom population experiment to ensure that
184 trace elements were present. The comparison of shell sizes of larvae kept in control ASW +
185 5% FSW or 100 % FSW yielded no significant differences ($p > 0.05$). Varying seawater $[\text{Ca}^{2+}]$
186 treatments were prepared by mixing ASW and CFSW (lowered $[\text{Ca}^{2+}]$) or by addition of CaCl_2
187 from a 500 mM stock solution to ASW (elevated $[\text{Ca}^{2+}]$). Following mixing, water samples
188 were taken and seawater $[\text{Ca}^{2+}]$ was measured using a flame photometer (EFOX 5053,
189 Eppendorf, Germany) calibrated with urine standards (Biorapid GmbH, Germany).

190 Seawater carbonate chemistry was manipulated by increasing alkalinity by addition of
191 $[\text{NaHCO}_3]$ to ASW or by lowering alkalinity by adding 1M HCl to the experimental units.
192 Excess CO_2 was removed by aeration of the experimental units for 30 min and embryos were
193 only added after pH had increased again to stable values (~ 7.8). Seawater pH was
194 determined on the NBS scale using a WTW 3310 pH meter equipped with a Sentix 81
195 electrode. Seawater C_T was determined using an AIRICA CO_2 analyzer and verified by
196 measuring certified reference material (Dickson et al. 2003). Seawater carbonate system
197 parameters (HCO_3^- , CO_3^{2-} , $\Omega_{\text{aragonite}}$) were calculated using the CO2SYS program with
198 KHSO_4 , K1 and K2 dissociation constants after Dickson et al. (1990) and Roy et al. (1993),
199 respectively. pH_{NBS} was converted to total scale pH. $\Omega_{\text{aragonite}}$ and $[\text{Ca}^{2+}][\text{HCO}_3^-]/[\text{H}^+]$ were
200 linearly adjusted according to measured seawater $[\text{Ca}^{2+}]$ (Table 2).

201

202 2.3 Microelectrode measurements of $[\text{Ca}^{2+}]$ in the calcifying space of D-stage veliger

203 Using ion-selective electrodes, Ca^{2+} gradients were measured in seawater and in the
204 calcification space (CS) below the surface of the shell in veliger larvae three days after
205 fertilization. The experimental set up and hardware was identical to that of Stumpp et al.
206 (2012), except for the addition of a metal plate connected to a water cooling system for
207 temperature control.

208 Borosilicate glass capillary tubes (inner diameter 1.2 mm, outer diameter, 1.5 mm) with
209 filament were pulled on a DMZ-Universal puller (Zeitz Instruments, Germany) to
210 micropipettes with tip diameters of 1-3 μm . Micropipettes were silanized with dimethyl
211 chlorosilane (Sigma-Aldrich, USA) in an oven at 200°C for 1h. Calcium sensitive liquid ion
212 exchangers (LIX) and LIX-PVC membranes were prepared according to de Beer et al. (2000)
213 with Ca^{2+} ionophore II (Sigma Aldrich). The microelectrodes were back filled with a KCl based
214 electrolyte (200 mM KCl, 2 mM $\text{CaCl}_2 \cdot 2\text{H}_2\text{O}$) and thereafter front loaded with LIX and finally
215 LIX-PVC at a length of 150 μm and 50 μm , respectively. To measure calcium in the CS,
216 larvae were placed into the temperature controlled perfusion chamber mounted on an
217 inverted microscope (Axiovert 135, Zeiss, Germany) at a density of 100 mL^{-1} and were held
218 in position using a holding pipette. The ion-selective probe was mounted on a remote-
219 controlled micro-manipulator and was introduced beneath the shell from the side of the

220 growing edge, where stable measurements were obtained within 5-10 seconds.
221 Microelectrode calibration was verified by measuring $[Ca^{2+}]$ of seawater standards as
222 described above and analogue outputs were channelled through an amplifier (WPI
223 Instruments, USA) to a chart recorder (Gould Instruments, USA).
224

225 2.4 Seawater $[Ca^{2+}]$ and carbonate chemistry of the Baltic Sea

226 Seawater $[Ca^{2+}]$ ($mM\ kg^{-1}$) was calculated for salinities between 3 and 20 $g\ kg^{-1}$ using the
227 correlation for chlorinities <4.5 and $>4.5\ g\ kg^{-1}$ provided by Kremling and Wilhelm (1997) and
228 a salinity-chlorinity conversion after Millero (1984). $[Ca^{2+}]$ was calculated for salinity values
229 measured in Kiel Fjord (N=4250, weekly measurements 2005-2009, 0-18 m, 54°19.8' N,
230 10°9.0' E, Clemmesen et al., unpublished, Casties et al. 2015) and at the Oder Bank
231 (N=260,000, hourly measurements, 2000-2015, 3+12 m water depths, 54°4.6' N, 14°9.6' E,
232 ~8 km off the *M. trossulus*-like collection site at Usedom (BSH 2000-2015, Table. 1). As
233 distribution of mytilid bivalves is limited by salinities below 4.5 $g\ kg^{-1}$ the calculation covers
234 the full $[Ca^{2+}]$ range relevant for mussels in this estuary (Westerbom et al. 2002). Carbonate
235 chemistry calculations are based on the salinity-alkalinity correlation published by Beldowski
236 et al. (2010) for salinities between 3 and 20 $g\ kg^{-1}$ and a seawater surface pCO_2 of 400 μatm
237 assuming equilibrium with current atmospheric CO_2 concentrations of ~400 ppm.
238 Calculations were performed for seawater temperatures of 15°C which corresponds to
239 average conditions experienced by larvae during the natural reproductive period from April to
240 June. The Baltic Sea has four sub areas which are differentially impacted by the inflow of
241 riverine freshwater and their respective chemical properties: the Central Baltic Sea with the
242 Kattegat transition area, the Gulf of Riga, the Gulf of Finland and the Bothnian Sea with Gulf
243 of Bothnia. Depending on the chemical properties of the riverine input, seawater carbonate
244 chemistry can differ substantially for similar salinity values between the four regions. The
245 same calculations were performed for predicting future conditions using atmospheric CO_2
246 concentration of 800 ppm.
247

248 2.5 Statistical analysis

249 All statistical analyses (t-test, Kruskal-Wallis test followed by Dunn's test, regression analysis,
250 linear and nonlinear model parameter fitting) were performed using R and the mosaic
251 package. Population comparisons were performed by fitting linear models for log transformed
252 data. Each experimental unit was considered as a replicate. Values in text and figures are
253 replicate means \pm standard error.
254

255 **3. Results**

256 3.1 PD I shell formation and CS $[Ca^{2+}]$ under varying seawater $[Ca^{2+}]$

257 Larval development until PD I formation was investigated for *M. edulis*-like collected in Kiel
258 Fjord. The lowest seawater $[Ca^{2+}]$ tested in the experiment was 0.51 mM which did not allow
259 successful development of larvae to the trochophore stage in the Kiel population and was
260 thus not considered in subsequent experiments. At all other $[Ca^{2+}]$ treatments, early
261 development was not adversely affected and larvae started to calcify prodossoconch I.
262 However, at $[Ca^{2+}]$ of <2 mM larvae were not able to produce a complete PD I shell. Even
263 after 7 days, shell size did not increase above a mean diameter of $63.7 \pm 6.0\ \mu m$ although
264 larvae stayed viable and continued to actively swim. In all other treatments, shells were fully
265 developed within 72 h post fertilization, but shell length declined linearly at $[Ca^{2+}]$ below 3
266 mM ranging between $104.5 \pm 2.1\ \mu m$ at 2.8 mM and $82.1 \pm 1.5\ \mu m$ at 1.6 mM, with significant
267 reductions below 2.5 mM $[Ca^{2+}]$ (H: 50.3, $p<0.001$, Dunn's test). Specimens kept at control
268 $[Ca^{2+}]$ of 4-5 mM had mean lengths of $108.2 \pm 2.5\ \mu m$. Modifications of seawater $[Ca^{2+}]$ in the
269 range 4-10 mM had only minor impacts on lengths and elevated $[Ca^{2+}]$ did not cause a
270 further increase of shell lengths above control size (Fig. 2a, Table 3a).

271 Results for shell formation rates of *M. edulis*-like larvae were compared with the *M. trossulus*-
272 like population from Usedom. Larvae were exposed to $[Ca^{2+}]$ between 0.4-5.8 mM (Fig. 2b,c).
273 Overall, the response curve for *M. trossulus*-like was similar to *M. edulis*-like (Table 3b).
274 Maximal shell sizes observed at 3.7 mM were $120 \pm 1.5\ \mu m$ and shell lengths started to

275 decline at lower $[Ca^{2+}]$. Nevertheless, at comparable $[Ca^{2+}]$ shell sizes were larger compared
276 to *M. edulis*-like and larvae were able to calcify a full PD I even at 1.1 mM $[Ca^{2+}]$ with an
277 average size of $81.9 \pm 3.2 \mu\text{m}$. In contrast, PD I formation was not completed at 0.4 mM, yet
278 larvae started to calcify. A linear model of the calcification response revealed a significant
279 effect of $[Ca^{2+}]$ and population on shell size but no interaction (Table 4a, Fig. 2c).

280 Microelectrode measurements of $[Ca^{2+}]$ in the CS of *M. edulis*-like revealed that CS $[Ca^{2+}]$
281 drops with seawater $[Ca^{2+}]$, (H: 21.2, $p < 0.01$, Fig. 3a). However, larvae kept at 3.5 mM $[Ca^{2+}]$
282 (above the critical $[Ca^{2+}]$ threshold) are characterized by CS $[Ca^{2+}]$ of 0.1 ± 0.01 mM above
283 seawater concentrations (paired t-test: $t = 16.9$, $p < 0.01$, Fig. 3b). In larvae raised at 2.6 and
284 2.3 mM $[Ca^{2+}]$, the difference between seawater and CS $[Ca^{2+}]$ declined to 0.06 ± 0.03 and
285 0.03 ± 0.02 mM which was not significantly enriched compared to the ambient seawater. In
286 contrast, the gradient between CS and seawater increased to 0.28 ± 0.02 mM in larvae
287 grown at 1.5 mM.

289 3.2 Combined effects of seawater $[Ca^{2+}]$ and carbonate chemistry on larval calcification

290 *M. edulis*-like larvae were exposed to a range of seawater $[Ca^{2+}]$ between 1 and 10 mM and
291 C_T concentrations between 880-3520 μM . PD I size was not modulated by increased
292 seawater C_T of 2900-3520 μM compared to control conditions (C_T : 1773 μM) and shell length
293 was only negatively affected by seawater $[Ca^{2+}]$ below 3 mM (Fig. 4a). In contrast, lowered
294 seawater C_T (975 μM) significantly affected shell formation and PD I length declined to $72.5 \pm$
295 $2.7 \mu\text{m}$ at control $[Ca^{2+}]$. Within these treatments shell length was marginally positively
296 correlated with seawater $[Ca^{2+}]$ but shell length remained reduced in all $[Ca^{2+}]$ treatments
297 (linear regression: $63 (\pm 2.2) \mu\text{m} + 2.9 (\pm 0.7) \times [Ca^{2+}]$, $F: 18.6$, $p < 0.01$, $R^2 = 0.47$, Fig. 4a).

298 Whereas, the correlation of shell length against $[Ca^{2+}]$ under reduced C_T differed significantly
299 from the three higher C_T treatments. Plotting PD I sizes against seawater $\Omega_{\text{Aragonite}}$ and
300 $[Ca^{2+}][HCO_3^-]/[H^+]$ revealed a similar correlation of calcification in all treatments (Fig. 4b, c).
301 Calcification of larvae started to decline at $\Omega_{\text{Aragonite}}$ below 1 with significant reductions in the
302 treatments with $\Omega_{\text{Aragonite}}$ below 0.5 (H: 44.5, $p < 0.001$, Dunn's test). Similarly, PD I size
303 declined at $[Ca^{2+}][HCO_3^-]/[H^+]$ values below 0.7 and shells were significantly smaller below
304 0.3 (H: 42.5, $p < 0.01$, Dunn's test). In addition, the shell formation responses of *M. edulis*-like
305 and *M. trossulus*-like to combined manipulations of $[Ca^{2+}]$ and carbonate chemistry were
306 more similar compared to the effects of lowered seawater $[Ca^{2+}]$ alone (Fig. 2c, 4b,c, Table
307 3b,c). Nevertheless, whereas the response to $\Omega_{\text{Aragonite}}$ was similar for both hybrid populations
308 they differed significantly in their response to $[Ca^{2+}][HCO_3^-]/[H^+]$ (Table 4c,d).

310 3.3 Calculation of seawater $[Ca^{2+}]$, Ω and $[Ca^{2+}][HCO_3^-]/[H^+]$ for the Baltic Sea

311 Calculations of seawater $[Ca^{2+}]$ were performed for the salinity range observed at the
312 collections sites of *M. edulis*-like and *trossulus*-like in Kiel Fjord and Usedom, respectively. In
313 Kiel Fjord, salinity fluctuated substantially between 10.5-24.7 g kg^{-1} in the period 2005 – 2009
314 which resulted in simultaneous strong variations of seawater $[Ca^{2+}]$ between 3.6 – 7.7 mM
315 with a mean of 5.6 mM (Table 1, Fig. 1d). In contrast, salinity in Usedom was lower with
316 mean salinity of 7.1 g kg^{-1} and, in absolute numbers, more stable (3.4-9.1 g kg^{-1} , Table 1).
317 Thus, seawater $[Ca^{2+}]$ in Usedom was ranging between 1.5 and 3.2 mM with an average of
318 2.7 mM (Table 1, Fig. 2d).

319 Calculation of $[Ca^{2+}]$ along the Baltic salinity gradient revealed that the critical concentrations
320 of 3 and 2.5 mM at which calcification is negatively affected are reached at a salinity of about
321 7-8 g kg^{-1} , respectively, in all four sub regions (Fig. 5a). In contrast, calculated values for
322 $[HCO_3^-]/[H^+]$ are above 0.13 in almost all regions within the distribution range of mussels as
323 long as the seawater is in equilibrium with current atmospheric CO_2 concentrations (Fig. 5b)
324 Only in the Gulf of Bothnia, critical values lower than 0.1 are observed for salinities of 4.5 g
325 kg^{-1} and below. For $\Omega_{\text{Aragonite}}$, undersaturation is observed at a salinity of 9 g kg^{-1} for the
326 central Baltic. The Gulfs of Bothnia and Finland are always undersaturated for $\Omega_{\text{Aragonite}}$, but
327 the Gulf of Riga seawater is supersaturated (Fig. 5c) and strong negative effects on larval
328 calcification can be expected for salinities of about 5 g kg^{-1} . Similarly, critical values for

329 $[\text{Ca}^{2+}][\text{HCO}_3^-]/[\text{H}^+]$ of 0.3 at which PD I formation is significantly affected are reached at a
330 salinity of 5 g kg^{-1} in most regions of the Baltic excluding the Gulf of Riga (Fig. 5d).
331 Conditions for calcification will become more adverse in future as atmospheric CO_2
332 concentrations are going to reach 800 ppm. In this scenario, critical values for $[\text{HCO}_3^-]/[\text{H}^+]$
333 will be observed in most areas of Baltic at salinities below 10 g kg^{-1} (Fig. 6b). In particular,
334 $[\text{Ca}^{2+}][\text{HCO}_3^-]/[\text{H}^+]$ and $\Omega_{\text{Aragonite}}$ will be below the critical threshold in all areas of the Baltic
335 Sea (Fig. 6c,d).

336

337 4. Discussion

338 This study investigated the impact of modifications of seawater $[\text{Ca}^{2+}]$ and carbonate
339 chemistry on shell formation of bivalve larvae. The experimental results were compared to
340 the environmental conditions prevailing in the Baltic Sea.

341 The laboratory experiments revealed that seawater $[\text{Ca}^{2+}]$ is a critical factor for shell
342 formation in marine bivalves. Similarly, Ca^{2+} deposition into the shells of *Crassostrea gigas*
343 larvae following PD I formation was similar at seawater $[\text{Ca}^{2+}]$ of 10 and 16.8 mM but
344 reduced by 40% at 6.1 mM (Maeda-Martinez 1987). Thus, where high oceanic $[\text{Ca}^{2+}]$ of ~ 10
345 mM is not limiting bivalve calcification the low concentrations present in estuaries such as the
346 Baltic, significantly affect biomineralization.

347 In both tested populations, *M. edulis*-like and *M. trossulus*-like the overall response curve
348 was similar and both populations become calcium limited at $[\text{Ca}^{2+}]$ below 3 mM. *M. trossulus*-
349 like appeared to be slightly more tolerant to lowered $[\text{Ca}^{2+}]$ as larvae maintained larger PD I
350 lengths at similar $[\text{Ca}^{2+}]$ and PD I formation was successfully accomplished at 1.1 mM. The
351 response matches seawater $[\text{Ca}^{2+}]$ observed in the respective habitats of the tested
352 populations and may result from either phenotypic plasticity or genetic adaptation. High
353 plasticity of PD I formation has been observed in transgenerational experiments when
354 parental animals were pre-exposed to elevated $p\text{CO}_2$ (Thomsen et al. 2017). Alternatively, it
355 is possible that *M. edulis*-like living in the western brackish Baltic may have already adapted
356 to lower $[\text{Ca}^{2+}]$ compared to populations and species living in habitats characterized by
357 higher $[\text{Ca}^{2+}]$ (Maeda-Martinez 1987). Gene flow between both tested populations is limited
358 since larval drift does not allow direct exchange (Stuckas et al. 2017). As PD I formation is a
359 crucial but sensitive stage during larval life, impaired calcification by low $[\text{Ca}^{2+}]$ can have
360 significant effects on larval performance and fitness. As the distribution of bivalves is
361 depending on successful larval dispersal, low $[\text{Ca}^{2+}]$ can be an important factor which
362 determines the distribution limits of mussels and represents a strong selective force.
363 Additionally, the strong $[\text{Ca}^{2+}]$ gradient observed between the western Baltic-Kattegat
364 transition zone and the central Baltic Sea can be one explanation for the simultaneously
365 observed allele frequency shift from *M. edulis*-like to *trossulus*-like (Larsson et al. 2016,
366 Stuckas et al. 2017).

367 Nevertheless, larval shell formation of Baltic mytilids starts to become $[\text{Ca}^{2+}]$ limited at
368 concentrations of about 3 mM and was significantly affected at 2.5 mM. Consequently, in
369 areas of the Baltic with salinities below $7\text{-}8 \text{ g kg}^{-1}$ and corresponding $[\text{Ca}^{2+}] < 3 \text{ mM}$, reduced
370 shell formation starts to compromise overall larval performance. At moderately lowered
371 $[\text{Ca}^{2+}] > 2 \text{ mM}$, shells were not malformed but calcification was only slowed down by a few
372 hours and larvae completed normal D-shell formation at later age. At the critical salinity of 4.5
373 g kg^{-1} which delineates the distribution boundary of mussels in the Baltic (Westerbom et al.
374 2002), $[\text{Ca}^{2+}]$ is as low as 1.8 mM whereby concentration below 2 mM substantially impaired
375 PD I formation in our experiments and did not allow production of a normal PD I. Importantly,
376 even under these adverse conditions larvae were viable and continued active swimming for
377 up to 7 days. Thus impaired calcification in low $[\text{Ca}^{2+}]$ seawater can result from two
378 mechanisms acting independently or in combination: I) continuous dissolution of existing
379 calcium carbonate crystals under highly corrosive conditions may prevent further net
380 calcification or II) larvae only use a pre-determined fraction of the energy stored in the egg
381 for calcification. If this amount is not sufficient to sustain full PD I formation under low $[\text{Ca}^{2+}]$
382 the budget does not seem to be adjusted to provide additional energy to complete
383 calcification. Instead larvae do not continue calcification and may switch to an energy saving

384 mode to stay alive. In our experiments, *M. trossulus*-like apparently developed a higher
385 tolerance to low $[Ca^{2+}]$ compared to *M. edulis*-like but incipient impairment of calcification at
386 about 3 mM was similar in both populations which suggests relatively conserved $[Ca^{2+}]$
387 transport mechanisms in both populations.

388 Impact of external $[Ca^{2+}]$ on calcification has previously been studied mostly in corals for
389 which a significant correlation was observed in a number of studies (e.g. Chalker 1976; Ip
390 and Krishnaveni 1991). Whereas cytosolic calcium concentration are tightly regulated and
391 kept constantly low, calcifiers obviously developed a mechanism to accumulate high $[Ca^{2+}]$ in
392 specialized compartments within or outside the cell for biomineralization. In corals, Ca^{2+}
393 uptake and transport to the site of calcification is driven by a combination of diffusive and
394 active transport and involves active transport by plasma membrane Ca^{2+} -ATPase (PMCA,
395 Tambutte et al. 1996; Barott et al. 2015). In bivalves, calcification is performed by the outer
396 mantle epithelium (OME) or the shell field in adults and larvae, respectively (Kniprath 1980),
397 and a PMCA homolog has been localized in the OME of oysters and its inhibition negatively
398 impacted shell growth in freshwater clams which might suggest a conserved function in
399 bivalve calcification as well (Wang et al. 2008; Zhao et al. 2016).

400 Early studies suggested that the extrapallial fluid (EPF) of bivalves provides the microhabitat
401 for calcification (Crenshaw 1972). However, $[Ca^{2+}]$ and acid-base status of bulk EPF of adult
402 mussels corresponds to seawater and haemolymph conditions, respectively, which supports
403 excretion of CO_2 via passive diffusion into the ambient seawater (Thomsen et al. 2010;
404 Heinemann et al. 2012). In *M. edulis*-like larvae, kept above the critical threshold of 3 mM,
405 CS $[Ca^{2+}]$ was marginally but significantly elevated compared to seawater $[Ca^{2+}]$. At lowered
406 environmental $[Ca^{2+}]$ between 2-3 mM CS $[Ca^{2+}]$ was not significantly enriched compared to
407 seawater concentration. At these seawater $[Ca^{2+}]$, calcification rates were significantly
408 reduced but larvae were still able to produce a smaller but complete PD I. At even lower
409 ambient $[Ca^{2+}]$ of 1.5 mM, CS $[Ca^{2+}]$ was again significantly elevated compared to seawater
410 which was, however, accompanied by strongly reduced PD I formation. The incapacity of
411 larvae to maintain transmembrane Ca^{2+} transport at lowered $[Ca^{2+}]$ potentially indicates a
412 significant contribution of diffusion or involvement of a low affinity Ca^{2+} transporter (e.g.
413 Na^+/Ca^{2+} Exchanger) in this process (Blaustein and Lederer 1999). Thus, larvae may actively
414 enrich CS $[Ca^{2+}]$ to increase $\Omega_{Aragonite}$ and support the structural integrity of the shell under
415 corrosive conditions. Alternatively, CS $[Ca^{2+}]$ only increased secondarily as a result of
416 drastically reduced calcification rates **caused by negative effects of low seawater $[Ca^{2+}]$ on**
417 **larval physiology.**

418 In addition to the sole effects of low Ca^{2+} availability, studies documented an influence of
419 varying Mg/Ca ratio on calcification for a range of marine organisms independent of absolute
420 $[Ca^{2+}]$ (reviewed in Ries et al. 2010). Considering 20-25 mM $[Mg^{2+}]$ present in the brackish
421 Baltic Sea, the Mg/Ca ratio in the experimental $[Ca^{2+}]$ treatments varied between about 2 and
422 20. Consequently not only Ca^{2+} limitation but also adverse Mg/Ca ratios may have had an
423 effect on PD I formation. Future research needs to perform manipulations of both ions under
424 **controlled conditions in order to investigate potential synergistic effects on larval calcification.**

425 In the present study, the effect of lowered $[Ca^{2+}]$ was most pronounced under conditions
426 when seawater carbonate chemistry was not a limiting parameter for calcification. Lowering
427 of seawater C_T , which has a similar effect on $\Omega_{Aragonite}$ and $[HCO_3^-]/[H^+]$ as acidification,
428 significantly affects the rate of PD I formation. Under these C_T / HCO_3^- limiting conditions,
429 seawater $[Ca^{2+}]$ had only a minor, yet slightly positive, linear effect on shell formation.
430 Presumably the effect was smaller as Ca^{2+} uptake was not any longer the only rate limiting
431 process but rather HCO_3^- uptake and / or H^+ extrusion (Bach 2015) or impaired kinetics of
432 crystal formation (Waldbusser et al. 2014).

433 Importantly, the applied experimental seawater manipulations of calcium and carbonate
434 chemistry can be integrated by calculation of $\Omega_{Aragonite}$ or extending the SIR term to
435 $[Ca^{2+}][HCO_3^-]/[H^+]$ which also takes lowered availability of $[Ca^{2+}]$ into account (Bach 2015;
436 Fassbender et al. 2016). Plotting shell length against these two parameters revealed a
437 similar response for all manipulations independent whether they were manipulated by
438 lowered $[Ca^{2+}]$ or C_T . The correlation of calcification with these parameters corresponded to

439 previously observed shell formation performance of mussels and oysters resulting from
440 modifications of seawater carbonate chemistry only (Waldbusser et al. 2014; Waldbusser et
441 al. 2015; Thomsen et al. 2015). As salinity and temperature were not changed in the
442 experiments performed with *M. edulis*-like $\Omega_{\text{Aragonite}}$ and $[\text{Ca}^{2+}][\text{HCO}_3^-]/[\text{H}^+]$ are linearly
443 correlated and it is not possible to distinguish whether shell formation is modified by the
444 changed kinetics of crystal formation (Waldbusser et al. 2015), higher dissolution due to
445 undersaturation of the EPF with respect to calcium carbonate (Miller et al. 2009; Thomsen et
446 al. 2010; Melzner et al. 2011, Frieder et al. 2017) or by lowered substrate availability and
447 impaired H^+ removal from the calcifying fluids (Thomsen et al. 2015; Bach 2015; Fassbender
448 et al. 2016). However, the calcification response of *M. trossulus*-like was similar to *M. edulis*-
449 like when plotted against $\Omega_{\text{Aragonite}}$ but differed significantly for $[\text{Ca}^{2+}][\text{HCO}_3^-]/[\text{H}^+]$ in
450 accordance with the higher tolerance to lowered $[\text{Ca}^{2+}]$. This could indicate local adaptation
451 of *M. trossulus*-like to the adverse environment in the low saline areas of the Baltic. In
452 contrast, the response to $\Omega_{\text{Aragonite}}$ was similar in animals from both populations which may
453 indicate that shell dissolution under corrosive conditions impacts net shell formation to the
454 same extent.

455 Our experimental data revealed that larval calcification is substantially compromised by
456 environmental conditions encountered in the Baltic Sea. Calculation of Baltic seawater $[\text{Ca}^{2+}]$
457 suggests $[\text{Ca}^{2+}]$ limitation of calcification at salinities of about 8 g kg^{-1} . Thus, with exception of
458 the western Baltic Sea with its higher salinity values, mussels inhabiting most areas of the
459 Baltic suffer from low Ca^{2+} availability. Interestingly, studies measuring Baltic Sea $[\text{Ca}^{2+}]$
460 revealed increasing concentrations over the last decades which may have a beneficial effect
461 on calcification for a given salinity (Kremling and Wilhelm 1997). Nevertheless, the expected
462 overall reduction of salinity will most likely exceed the minor positive effect of $[\text{Ca}^{2+}]$
463 enrichment and negatively affect overall fitness by osmotic stress and secondarily
464 calcification (Gräwe et al. 2013).

465 In contrast to $[\text{Ca}^{2+}]$, estimating current carbonate chemistry for the four Baltic sub regions
466 suggests that the influence is of less importance for limitation of calcification. The calculated
467 $[\text{HCO}_3^-]/[\text{H}^+]$ and $\Omega_{\text{Aragonite}}$ for seawater in equilibrium with current atmospheric CO_2
468 concentrations remain above the critical thresholds of 0.1-0.13 and 1, respectively (Thomsen
469 et al. 2015, this study). However, this conclusion does not consider the substantial variability
470 of carbonate chemistry in the surface water of the Baltic which is modified by biogeochemical
471 processes such as riverine composition, photosynthesis and upwelling on a seasonal and
472 spatial scale. Seawater carbonate chemistry can be substantially modified by phytoplankton
473 blooms in spring and early summer causing a draw down of seawater $p\text{CO}_2$ to $150 \mu\text{atm}$
474 thereby causing elevated pH, $[\text{CO}_3^{2-}]$ and $[\text{HCO}_3^-]/[\text{H}^+]$ for several weeks (Schneider and
475 Kuss 2004). Consequently, larvae can be exposed to environmental conditions which are
476 beneficial for calcification. In contrast, local upwelling phenomena have the opposite effect
477 leading to lowered pH and $[\text{CO}_3^{2-}]$, $[\text{HCO}_3^-]/[\text{H}^+]$ and elevated $p\text{CO}_2$ (Thomsen et al. 2010;
478 Saderne et al. 2013). Upwelling events are common in the Baltic Sea in particular along the
479 western coastlines (Myrberg and Andrejev 2003). However, research mostly focused on the
480 effect of upwelling on temperature and nutrient supply but neglected the local impacts on
481 carbonate chemistry (e.g. Haapala 1994). As upwelling causes rapid elevation of $p\text{CO}_2$ within
482 a short period of hours but can last for several days to few weeks, thus for a significant part
483 of a larval life time, its impact on calcification and performance of larvae can be substantial
484 (Barton et al. 2012; Thomsen et al. 2015, 2017).

485 In addition to the present carbonate system variability, the successive increase of
486 atmospheric CO_2 concentrations and coupled pH decline in the Baltic will result in
487 progressively adverse conditions for calcification. This process is particularly critical for
488 mussel populations inhabiting the low saline areas of the Baltic where conditions for
489 calcification are less favourable already today and will become more adverse in the future.
490 Nevertheless, it has recently been shown that increasing A_T (from an unaccounted source)
491 may partly and even completely compensate the negative effects of CO_2 uptake (Müller et al.
492 2016). Consequently, bivalve calcification may benefit from higher A_T and thus favourable
493 carbonate chemistry in future, but lowered salinity might still affect performance.

494 Both substrates relevant for calcification, Ca^{2+} and inorganic carbon are integrated in the
495 terms Ω and the SIR extended to $[\text{Ca}^{2+}][\text{HCO}_3^-]/[\text{H}^+]$. In fact the calcification response of
496 bivalve larvae in our experiments was accurately described by both terms for a given salinity
497 and temperature. Nevertheless, calculations of the environmental conditions in the four Baltic
498 sub regions revealed important differences. $\Omega_{\text{Aragonite}}$ remains favourable for calcification (>1)
499 in most parts of the central Baltic and in the Gulf of Riga caused by high alkaline riverine
500 runoff and therefore prohibits dissolution of shell crystals (Juhna and Klavins 2000). In
501 contrast, calculated values for $[\text{Ca}^{2+}][\text{HCO}_3^-]/[\text{H}^+]$ are below the critical threshold of 0.7 in all
502 sub regions at a salinity of 11 g kg^{-1} caused by low $[\text{Ca}^{2+}]$. Thus, it is of high ecological
503 relevance whether bivalve calcification is sensitive to the reduced kinetic of shell formation
504 and dissolution depending on Ω or lowered substrate availability and inhibition by $[\text{H}^+]$.
505 According to our experimental data most likely a combination of both parameters is
506 determining sensitivity. However, compared to *M. edulis*-like, *M. trossulus*-like seems to have
507 evolved a slightly higher tolerance to low $[\text{Ca}^{2+}][\text{HCO}_3^-]/[\text{H}^+]$, but not to low $\Omega_{\text{Aragonite}}$. A similar
508 response has been observed in a comparison between Baltic and North Sea mussels under
509 simulated ocean acidification (Thomsen et al. 2017).
510 In conclusion, this study reveals strong impacts of lowered $[\text{Ca}^{2+}]$ and carbonate chemistry,
511 which are naturally changing along the Baltic salinity gradient, on the early calcification of
512 mussel larvae. Strong delays and impairment of complete shell formation most likely affect
513 the energy budget and overall physiology of mussels in the low saline areas. Consequently,
514 low $[\text{Ca}^{2+}]$ and adverse carbonate chemistry impact mussel fitness substantially and
515 therefore likely seem to contribute significantly in determining the distribution of marine
516 mussels in estuaries such as the Baltic Sea.

517 518 **Author Contributions:**

519 JT conceived the study and led the writing of the manuscript; JT, KR, TS and FM collected
520 data; JT, KR, MB, and FM analysed the data. All authors contributed to the various
521 manuscript drafts.

522 523 **Acknowledgements:**

524 The authors thank Thomas Stegmann for performing Ca^{2+} measurements, Marian Hu for
525 supporting Ca^{2+} -microelectrode measurements and Ulrike Panknin for maintaining
526 *Rhodomonas* cultures. Furthermore, Detlev Machoczek and Rainer Kiko are acknowledged
527 for providing and supporting processing of Oder Bank salinity data, respectively. This study
528 was funded by the BMBF program BIOACID subproject 2.3 and CACHE, a Marie Curie Initial
529 Training Network (ITN) funded by the People Programme (Marie Curie Actions) of the
530 European Union's Seventh Framework Programme FP7/2007-2013/ under REA grant
531 agreement n°[605051]13. The authors declare no conflict of interest.

532 533 **Data availability:**

534 All data are available under: Thomsen, Jörn; Ramesh, Kirti; Sanders, Trystan; Bleich, Markus;
535 Melzner, Frank (2017): Effects of seawater calcium on calcification in mussel larvae.
536 PANGAEA, Unpublished dataset #871804.

537 538 **References:**

539 Bach, L.T.: The role of carbonate ion concentration for the production of calcium carbonate
540 by marine organisms, *Biogeosciences*, 12, 4939-4951, 2015.
541
542 Barott, K.L., Perez, S.O., Linsmayer, L.B., and Tresguerres, M.: Differential localization of ion
543 transporters suggests distinct cellular mechanisms for calcification and photosynthesis
544 between two coral species. *Am. J. Physiol. Reg. I.*, 309, R235-R246, 2015.
545
546 Barton, A., Hales, B., Waldbusser, G.G., Langdon, C., and Felly, R.A.: The Pacific oyster
547 *Crassostrea gigas*, shows negative correlation to naturally elevated carbon dioxide levels:
548 Implications for near-term ocean acidification effects. *Lim. Oceanog.*, 57, 698-710, 2012.

549
550 Beldowski, J., Löffler, A., and Joensuu, L.: Distribution and biogeochemical control of total
551 CO₂ and total alkalinity in the Baltic Sea. *J. Mar. Syst.*, 81, 252–259, 2010.
552
553 Blaustein, M.P., and Lederer W.J., Sodium/Calcium Exchange: Its physiological implications.
554 *Physiological Reviews*, 79, 763-854, 1999.
555
556 BSH: Hourly meteorological observations at Station Oder Bank 2000-2015, Bundesamt für
557 Seeschifffahrt und Hydrographie, Hamburg
558
559 Casties, I., Clemmensen, C., Melzner, F., and Thomsen, J.: Salinity dependence of
560 recruitment success of the sea star *Asterias rubens* in the brackish western Baltic Sea.
561 *Helgoland Mar. Res.*, 69, 169-175, 2015.
562
563 Chalker, B.E.: Calcium transport during skeletogenesis in hermatypic corals, *Comp. Biochem.*
564 *Physiol. A*, 54, 455-459, 1976.
565
566 Cragg, S.M.: The adductor and retractor muscles of the veliger of *Pecten maximus* (L.)
567 (*Bivalvia*), *J. Mollus. Stud.*, 51, 276-283, 1985.
568
569 Crenshaw, M.A.: The inorganic composition of molluscan extrapallial fluid, *Biol. Bull.*, 143,
570 506-512, 1972.
571
572 Cyronak, T., Schulz, K.G., and Jokiel, P.L.: The Omega myth: what really drives lower
573 calcification rates in an acidifying ocean, *ICES J. Mar. Sci.*, 73, 558-562, 2015.
574
575 De Beer, D., Köhl, M., Stambler, N., and Vaki, L.: A mirosensor study of light enhanced Ca²⁺
576 uptake and photosynthesis in the reef-building hermatypic coral *Favia* sp., *Mar. Ecol. Prog.*
577 *Ser.*, 194, 75-85, 2000.
578
579 Dickson, A.G.: Standard potential of the reaction – AgClS+1/2 H₂ = AgS+HClAq and the
580 standard acidity constant of the ion HSO₄ – in synthetic sea-water from 273.15-K to 318.15-
581 K, *J. Chem. Thermodyn.*, 22, 113–127, 1990.
582
583 Dickson, A.G., Afghan, J.D., and Anderson, G.G.: Reference materials for oceanic CO₂
584 analysis: A method for the certification of total alkalinity. *Mar. Chem.*, 80, 185-197, 2003.
585
586 Enderlein, P., and Wahl, M.: Dominance of blue mussels versus consumer-mediated
587 enhancement of benthic diversity, *J. Sea Res.*, 51, 145-155, 2004.
588
589 Falini, G, Albeck, S, Weiner, S, and Addadi, L.: Control of aragonite or calcite polymorphism
590 by mollusk shell macromolecules, *Science*, 271, 67-69, 1996.
591
592 Fassbender, A.J., Sabine, C.L., and Feifel, K.M.: Consideration of coastal carbonate
593 chemistry in understanding biological calcification. *Geophys. Res. Lett.*, 43, 4467-4476, 2016.
594
595 Frieder, C.A., Applebaum, S.L., Pan, T.C.F., Hedgecock, D., and Manahan, D.: Metabolic
596 cost of calcification in bivalve larvae under experimental ocean acidification. *ICES J. Mar.*
597 *Sci.*, 74, 941-954, 2017.
598
599 Gazeau, F., Parker, L.M., Comeau, S., Gattuso, J.P., O`Connor, W.A., Martin, S., Pörtner, H.
600 O., and Ross, P.M.: Impacts of ocean acidification on marine shelled molluscs. *Mar. Biol.*,
601 160, 2207-2245, 2013.
602

603 Gräwe, U., Freidland, R., and Burchard, H.: The future of the western Baltic Sea: two
604 possible scenarios, *Ocean Dynam.*, 63, 901-921, 2013.
605

606 Gustafsson, E., Wällstedt, T., Humborg, C., Mörrth, C.M., and Gustafsson, B.G.: External total
607 alkalinity loads versus internal generation: The influence of nonriverine alkalinity sources in
608 the Baltic Sea, *Global Biochem. Cy.*, 28, 1358-1370, 2014.
609

610 Haapala, J.: Upwelling and its influence on nutrient concentration in the coastal area of the
611 Hanko Peninsula, Entrance of the Gulf of Finland, *Estuar. Coast. Shelf S.*, 38, 507-521, 1994.
612

613 Haynert, K., Schönfeld, J., Schiebel, R., Wilson, B., and Thomsen, J.: Response of benthic
614 foraminifera to ocean acidification in their natural sediment environment: a long-term
615 culturing experiment, *Biogeosciences*, 11, 1581–1597, 2014.
616

617 Heinemann, A., Fietzke, J., Melzner, F., Böhm, F., Thomsen, J., Garbe-Schönberg, D. and
618 Eisenhauer, A.: Conditions of *Mytilus edulis* extracellular body fluids and shell composition in
619 a pH-treatment experiment: Acid-base status, trace elements and $\delta^{11}\text{B}$, *Geochem. Geophys.*
620 *Geosy.*, 13, Q01005, 2013.
621

622 Ip, Y.K., and Krishnaveni, P.: Incorporation of Strontium ($^{90}\text{Sr}^{2+}$) into the skeleton of the
623 hermatypic coral *Galaxea fascicularis*, *J. Exp. Zool.*, 258, 273-276, 1991.
624

625 Johannesson, K., Smolarz, K., Grahn, M., and Andre, C.: The Future of Baltic Sea
626 Populations: Local Extinction or Evolutionary Rescue? *AMBIO*, 40, 179-190, 2011.
627

628 Juhna, T., and Klavins, M.: Water-quality changes in Latvian and Riga 1980-2000:
629 Possibilities and Problems, *AMBIO*, 30, 306-314, 2001.
630

631 Kester, D.R., Duedall, I.W., Connors, D.N., and Pytkowicz, R.M.: Preparation of artificial
632 seawater, *Limnol. Oceanogr.*, 12, 176-179, 1967.
633

634 Kniprath, E.: Larval development of the shell and the shell gland in *Mytilus* (Bivalvia). *Roux's*
635 *Arch. Dev. Biol.*, 188, 201-204, 1980.
636

637 Kremling, K., and Wilhelm, G.: Recent increase of the calcium concentrations in Baltic Sea
638 waters. *Mar. Pollut. Bull.*, 34, 763-767, 1997.
639

640 Kube, S., Gerber, A., Jansen, J.M., and Schiedek, D.: Patterns of organic osmolytes in two
641 marine bivalves, *Macoma baltica*, and *Mytilus* spp., along their European distribution, *Mar.*
642 *Biol.*, 149, 1387-1396, 2006.
643

644 Lucas, A., and Rangel, C.: Detection of the first larval feeding in *Crassostrea gigas* using the
645 epifluorescence microscope, *Aquaculture*, 30, 369-374, 1983.
646

647 Maar, M., Saurel, C., Landes, A., Dolmer, P., and Petersen, J.K.: Growth potential of blue
648 mussels (*M. edulis*) exposed to different salinities evaluated by a Dynamic Energy Budget
649 model, *J. Mar. Sys.*, 148, 48-55, 2015.
650

651 Maeda-Martinez, A.N.: The rates of calcium deposition in shells of molluscan larvae, *Comp.*
652 *Biochem. Physiol. A*, 86, 21-28, 1987.
653

654 Malone, P.G., and Dodd, J.R.: Temperature and salinity effects on calcification rate in *Mytilus*
655 *edulis* and its paleoecological implications, *Limnol. Oceanogr.*, 12, 432-436, 1965.
656

657 Martin, G., Kotta, J., Möller, T., and Herkül, K.: Spatial distribution of marine benthic habitats
658 in the Estonian coastal sea, northeastern Baltic Sea. *Est. J. Ecol.*, 62, 165-191, 2013.
659

660 McConnaughey T.A., and Gillikin, D.P.: Carbon isotopes in mollusk shell carbonates, *Geo-*
661 *Mar. Lett.*, 28, 287–299, 2008.
662

663 Meier, H.E.M., Kjellström, E., and Graham, L.P.: Estimating uncertainties of projected Baltic
664 Sea salinity in the late 21st century, *Geophys. Res. Lett.*, 33, L15705, 2006.
665

666 Melzner, F., Stange, P., Trübenbach, K., Thomsen, J., Casties, I., Panknin, U., Gorb, S., and
667 Gutowska, M.A.: Food supply and seawater pCO₂ impact calcification and internal shell
668 dissolution in the Blue Mussel *Mytilus edulis*, *PLOS ONE*, 6, e24223, 2011.
669

670 Melzner, F., Thomsen, J., Koeve, W., Oschlies, A., Gutowska, M.A., Bange, H. W., Hansen,
671 H.P., and Körtzinger, A.: Future ocean acidification will be amplified by hypoxia in coastal
672 habitats, *Mar. Biol.*, 160, 1875-1888, 2013.
673

674 Miller, A.W., Reynolds, A.C., Sobrino, C., and Riedel, G.F.: Shellfish face uncertain future in
675 high CO₂ world: Influence of acidification on oyster larvae calcification and growth in
676 estuaries, *PLOS ONE*, 4, e5661, 2009.
677

678 Millero, F.: The conductivity-density-salinity-chlorinity relationships for estuarine water,
679 *Limnol. Oceanogr.*, 29, 1317-1321, 1984.
680

681 Mucci, A.: The solubility of calcite and aragonite in seawater at various salinities,
682 temperatures, and one atmosphere total pressure. *Am. J. Sci.*, 28, 780-799, 1983.
683

684 Müller, J., Schneider, B., and Rehder, G.: Long-term alkalinity trends in the Baltic Sea and
685 implications for Co₂-induced acidification, *Limnol. Oceanogr.*, 61, 1984-2002, 2016.
686

687 Myrberg, K., and Andrejev, O.: Main upwelling regions in the Baltic Sea - a statistical analysis
688 based on three-dimensional modelling, *Boreal Environ. Res.*, 8, 97-112, 2003.
689

690 Natochin, Y.V., Berger, V.Y., Khlebovich, V.V., Lavrova, E.A., and Michailova, O.Y.: The
691 participation of electrolytes in adaptation mechanisms of intertidal molluscs' cells to altered
692 salinity. *Comp. Biochem. Physiol. A*, 63, 115-119, 1979.
693

694 Ohlson, M., and Anderson, L.: Recent investigation of total carbonate in the Baltic Sea:
695 changes from the past as a result of acid rain? *Mar. Chem.*, 30, 259-267, 1990.
696

697 Podbielski, I., Bock, C., Lenz, M., and Melzner, F.: Using the critical salinity (S_{crit}) concept to
698 predict invasion potential of the anemone *Diadumene lineata* in the Baltic Sea, *Mar. Biol.*,
699 163, 227, 2016.
700

701 Ries, J.B., Review: geological and experimental evidence for secular variation in seawater
702 Mg/Ca (calcite-aragonite seas) and its effects on marine biological calcification,
703 *Biogeosciences*, 7, 2795–2849, 2010.
704

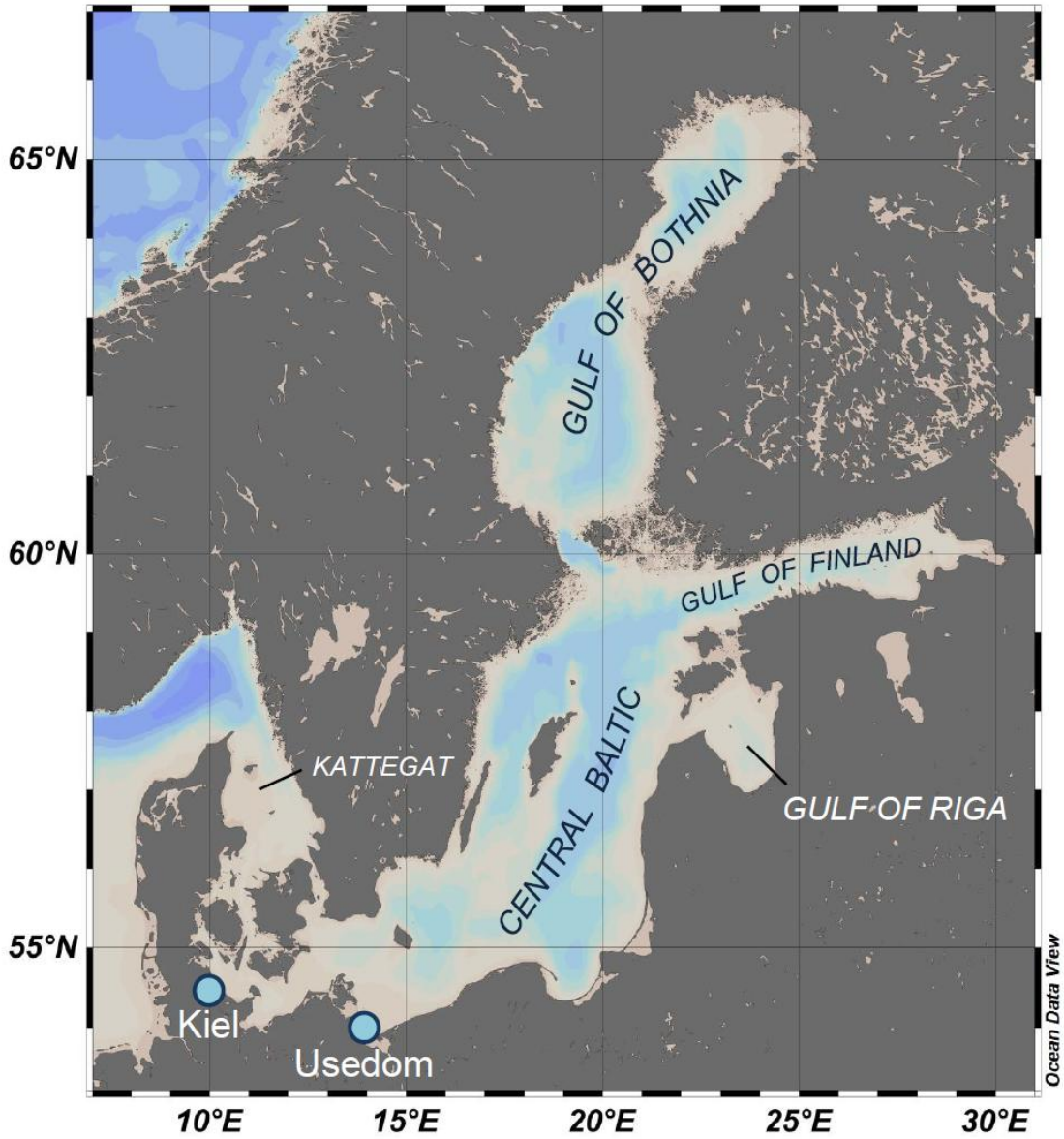
705 Riisgard, H.U., Larsen, P. S., Turja, R., and Lundgreen, K.: Dwarfism of blue mussels in the
706 lower saline Baltic Sea – growth to the lower salinity limit, *Mar. Ecol. Prog. Ser.*, 517, 181-
707 192, 2014.
708

709 Roy, R.N., Roy, L.N., Vogel, K.M., Porter-Moore, C., Pearson, T., Good, C.E., Millero, F. J.,
710 and Campbell, D.: The dissociation constants of carbonic acid in seawater at salinities 5 to
711 45 and temperatures 0 to 45°C. *Mar. Chem.*, 44, 249-267, 1993.

712
713 Saderne, V., Fietzek, P., and Herman, P.M.J.: Extreme variations of pCO₂ and pH in a
714 macrophyte meadow of the Baltic Sea in summer: Evidence of the effect of photosynthesis
715 and local upwelling, PLOS ONE, 8, e62689, 2013.
716
717 Schneider, B., and Kuss, J.: Past and present productivity of the Baltic Sea inferred from
718 pCO₂ data. Cont. Shelf Res., 24, 1611-1622, 2004.
719
720 Silva, A.L. and Wright, S.H.: Short-term cell volume regulation in *Mytilus californianus* gill, J.
721 Exp. Biol., 194, 47-68, 1994.
722
723 Stuckas, H., Knobel, L., Schade, H., Breusing, C., Hinrichsen, H.-H., Bartel, M., Langguth, K.
724 and Melzner, F.: Combining hydrodynamic modelling with genetics: Can passive larval
725 drift shape the genetic structure of Baltic *Mytilus* populations? Mol. Ecol., 26, 2765-2782,
726 2017.
727
728 Stumpp, M., Hu., M., Casties, I., Saborowski, R., Bleich, M., Melzner, F., and Dupont, S.:
729 Digestion in sea urchin larvae impaired under ocean acidification, Nature Clim. Change, 3,
730 1044-1049, 2013.
731
732 Tambutte, E., Allemand, D., Mueller, E. & Jaubert, J.: A compartmental approach to the
733 mechanism of calcification in hermatypic corals. J. Exp. Biol., 199, 102-1041 1996.
734
735 Thomsen, J., Gutowska, M.A., Saphörster, J., Heinemann, A., Trübenbach, K., Fietzke, J.,
736 Hiebenthal, C., Eisenhauer, A., Körtzinger, A., Wahl, M., and Melzner, F.: Calcifying
737 invertebrates succeed in a naturally CO₂-rich coastal habitat but are threatened by high
738 levels of future acidification, Biogeosciences, 7, 3879–3891, 2010.
739
740 Thomsen, J., Haynert, K., Wegner, K. M., and Melzner, F.: Impact of seawater carbonate
741 chemistry on the calcification of marine bivalves, Biogeosciences, 12, 4209-4220, 2015.
742
743 Thomsen, J., Stapp, L.S., Haynert, K., Schade, H., Danelli, M., Lannig, G., Wegner, K.M.,
744 and Melzner, F.: Naturally acidified habitat selects for ocean acidification–tolerant mussels,
745 Sci. Adv., 3, e1602411, 2017.
746
747 Waldbusser, G.G., Brunner, E.L., Haley, B.A., Hales, B., Langdon, C.J., and Prah, F. G.: A
748 developmental and energetic basis linking larval oyster shell formation to acidification
749 sensitivity, Geophys. Res. Lett., 40, 1–6, 2013.
750
751 Waldbusser, G.G., Hales, B., Langdon, C.J., Haley, B.A., Schrader, P., Brunner, E.L., Gray.
752 M.W., Miller, C.A., and Gimenez, I.: Saturation-state sensitivity of marine bivalve larvae to
753 ocean acidification, Nature Clim. Change, 5, 273-280, 2014.
754
755 Waldbusser, G.G., Hales, B., Langdon, C.J., Haley, B.A., Schrader, P., Brunner, E.L., Gray.
756 M.W., Miller, C.A., Gimenez, I., and Hutchinson, G.: Ocean acidification has multiple modes
757 of action in bivalve larvae, PLOS ONE, 10, e0128376, 2015.
758
759 Wang, X., Fan, W., Xie, L., and Zhang, R.: Molecular cloning and distribution of a plasma
760 membrane calcium ATPase homolog from the pearl oyster *Pinctada fucata*, Tsinghua Sci.
761 Technol., 13, 439-446, 2008.
762
763 Westerborn, M., Kilpi, M., and Mustonen, O.: Blue mussels, *Mytilus edulis*, at the edge of the
764 range: population structure, growth and biomass along a salinity gradient in the north-eastern
765 Baltic Sea, Mar. Biol., 140, 991-999, 2002.
766

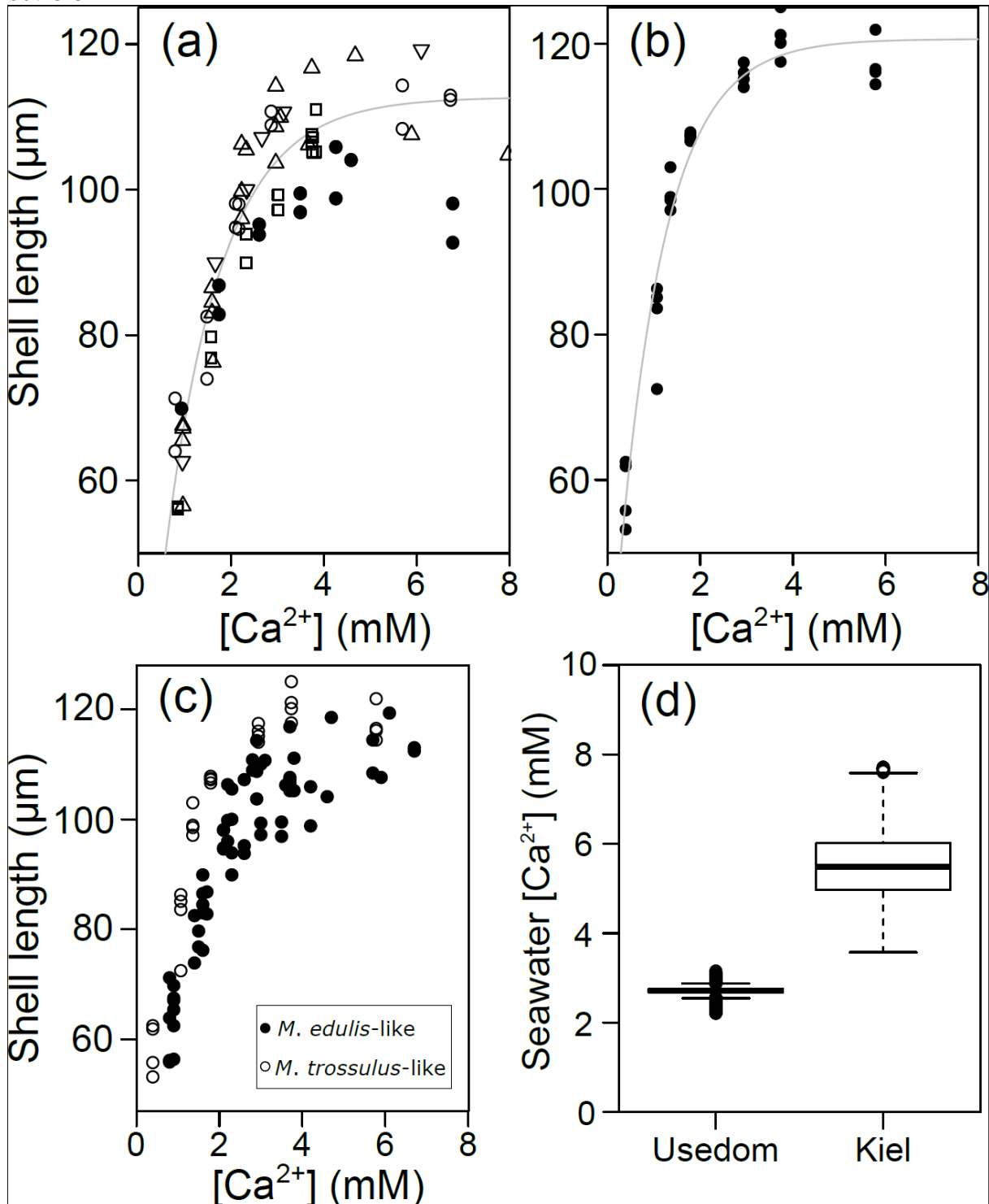
767 Whitfield, A.K., Elliott, M., Basset, A., Blaber, S.J.M., and West, R.J.: Paradigms in estuarine
768 ecology – A review of the Remane diagram with a suggested revised model for estuaries,
769 Estuar. Coast. Shelf S., 97, 78-90, 2012.
770
771 Williams, E.K., and Hall, J.A.: Seasonal and geographic variability in toxicant sensitivity of
772 *Mytilus galloprovincialis*, Australas. J. Ecotox., 5, 1-10, 1999.
773
774 Willmer, P.G.: Sodium fluxes and exchange pumps: Further correlates of osmotic conformity
775 in the nerves of an estuarine bivalve (*Mytilus edulis*). J. Exp. Biol., 77, 207-223, 1978).
776
777 Wright, S.H., Moon, D.A., and Silva, A.L.: Intracellular Na⁺ and the control of amino acid
778 fluxes in the integumental epithelium of a marine bivalve, J. Exp. Biol., 142. 293-310, 1989.
779
780 Zhao, L., Schöne, B.R., and Mertz-Kruas, R.: Delineating the role of calcium in shell
781 formation and elemental composition of *Corbicula fluminea* (Bivalvia), Hydrobiologica, 790,
782 259-270, 2016.
783
784
785
786
787
788
789
790
791
792
793
794
795
796
797
798
799
800
801
802
803
804
805
806
807
808
809
810
811
812
813
814
815
816
817
818
819
820
821

822 Fig. 1 Bathymetric map of the Baltic Sea and its sub regions which are characterized by
823 specific carbonate chemistry. Sampling spots for mussel populations used in the experiments
824 are indicated by light blue dots.



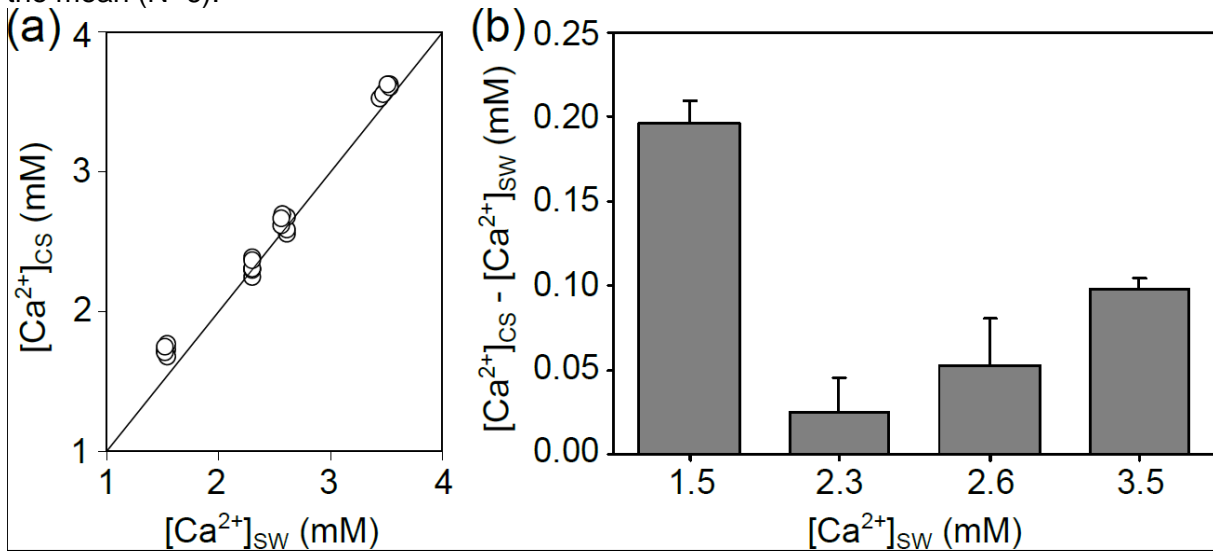
825
826
827
828
829
830
831
832
833
834
835
836
837
838
839
840

841 Fig. 2 Prodissoconch I length of mussel larvae as a function of seawater $[Ca^{2+}]$. a) *M. edulis*-
 842 like, different symbols represent different experimental runs (1-5) b) *M. trossulus*-like, c)
 843 Comparison of *M. edulis*-like and *trossulus*-like, d) Boxplots of seawater $[Ca^{2+}]$ at the
 844 collection site in Kiel Fjord and at Usedom depicting median, 25 and 75% quartiles and
 845 outliers.



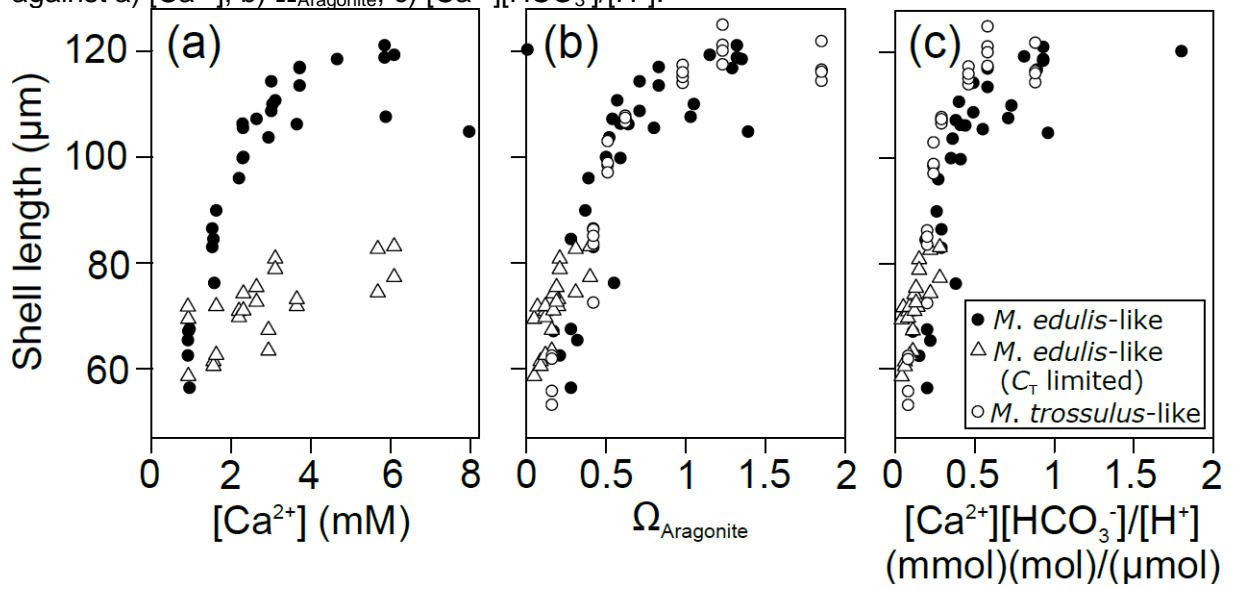
846
 847
 848
 849
 850
 851
 852

853 Fig. 3 $[Ca^{2+}]$ in the calcifying space (CS) of *M. edulis*-like larvae reared under control
 854 conditions (3.5 mM) and lower seawater $[Ca^{2+}]$. a) CS $[Ca^{2+}]$ as a function of seawater $[Ca^{2+}]$,
 855 the line indicates the isoline. b) Difference between CS $[Ca^{2+}]$ and seawater $[Ca^{2+}]$ at four
 856 $[Ca^{2+}]$ treatments expressed as $[Ca^{2+}]_{CS} - [Ca^{2+}]_{SW}$. Bar chart depicts mean \pm standard error of
 857 the mean (N=6).



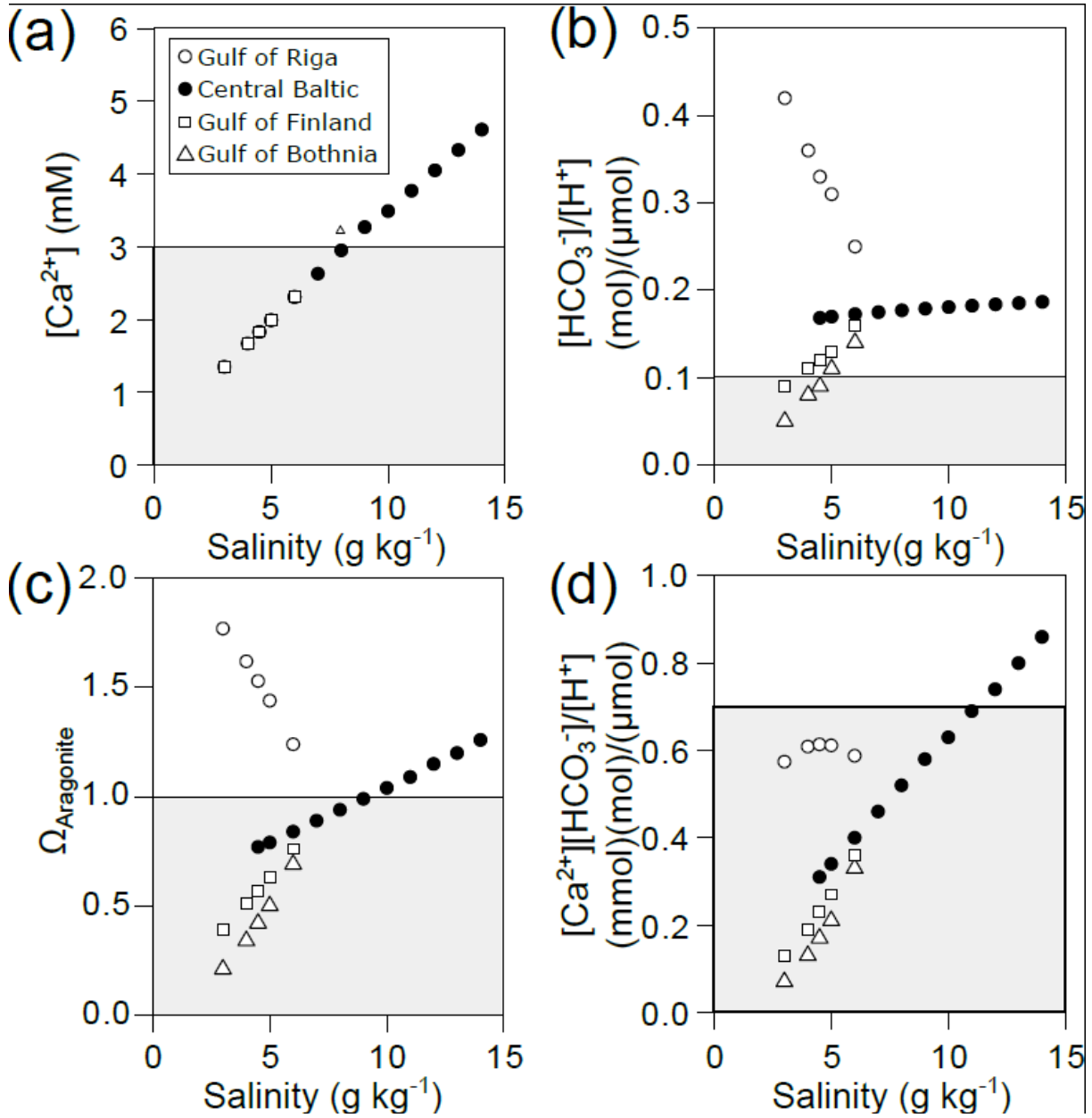
858
 859
 860
 861
 862
 863
 864
 865
 866
 867
 868
 869
 870
 871
 872
 873
 874
 875
 876
 877
 878
 879
 880
 881
 882
 883
 884
 885
 886
 887
 888
 889
 890
 891
 892

893 Fig. 4 Prodissoconch I length of mussel larvae exposed to varying C_T and $[Ca^{2+}]$ plotted
 894 against a) $[Ca^{2+}]$, b) $\Omega_{Aragonite}$, c) $[Ca^{2+}][HCO_3^-]/[H^+]$.



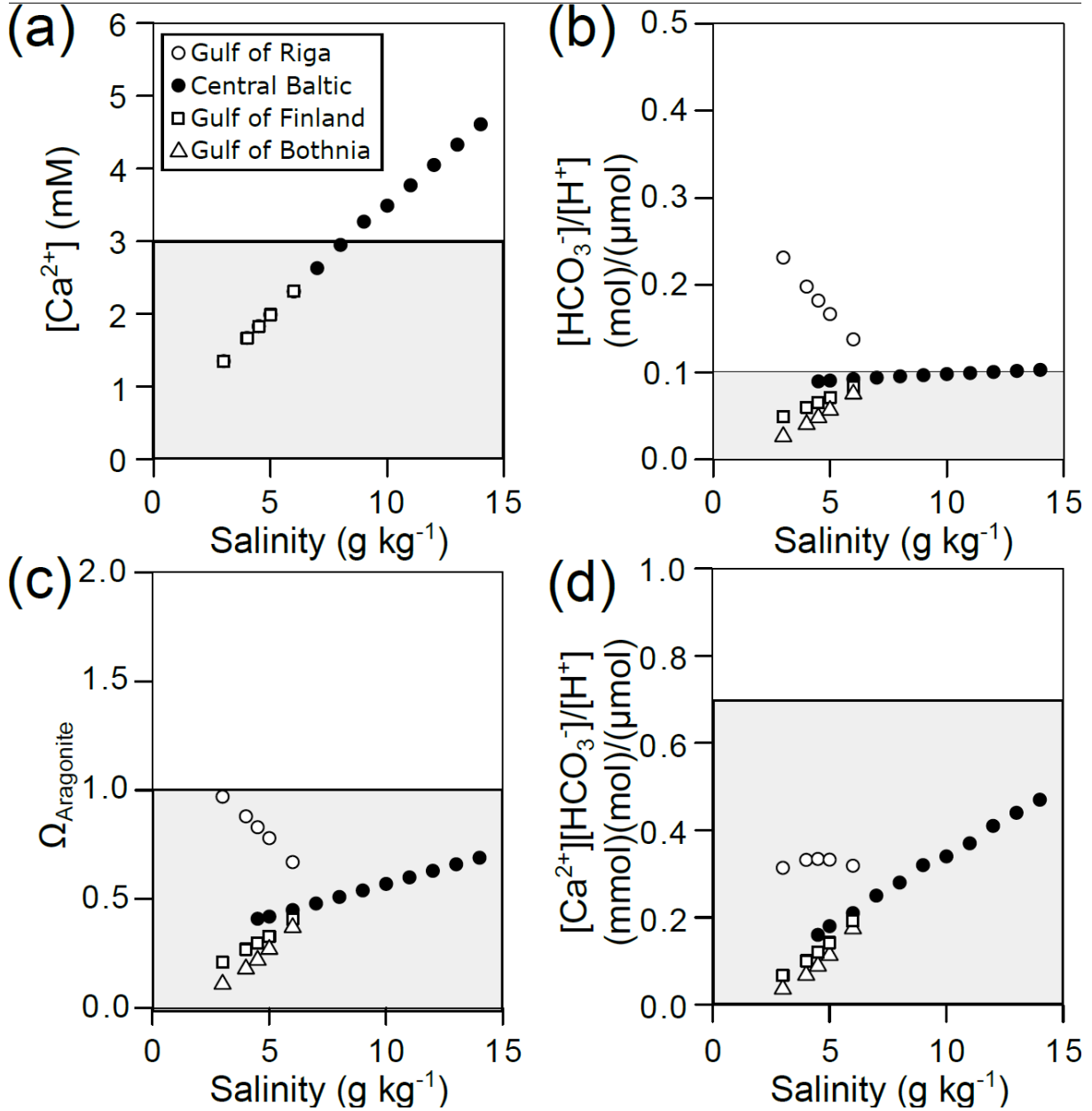
895
 896
 897
 898
 899
 900
 901
 902
 903
 904
 905
 906
 907
 908
 909
 910
 911
 912
 913
 914
 915
 916
 917
 918
 919
 920
 921
 922
 923
 924
 925
 926
 927
 928
 929
 930
 931

932 Fig. 5 Environmental parameters relevant for calcification in the Baltic Sea calculated for
 933 current salinity- A_T correlations and atmospheric CO_2 concentration (400 ppm). a) $[Ca^{2+}]$, b)
 934 $[HCO_3^-]/[H^+]$, c) $\Omega_{Aragonite}$ and d) $[Ca^{2+}][HCO_3^-]/[H^+]$ plotted against salinity for the four sub
 935 regions of the Baltic Sea. Grey areas indicate conditions of incipient reduction of larval
 936 calcification rates.



937
 938
 939
 940
 941
 942
 943
 944
 945
 946
 947
 948
 949
 950
 951

952 Fig. 6 Predicted environmental parameters relevant for calcification in the Baltic Sea
 953 calculated for current salinity- A_T correlations and future atmospheric CO_2 concentration (800
 954 ppm). a) $[Ca^{2+}]$, b) $[HCO_3^-]/[H^+]$, c) $\Omega_{Aragonite}$ and d) $[Ca^{2+}][HCO_3^-]/[H^+]$ plotted against salinity
 955 for the four sub regions of the Baltic Sea. Grey areas indicate conditions of incipient
 956 reduction of larval calcification rates.
 957



958
 959
 960
 961
 962
 963
 964
 965
 966
 967
 968
 969
 970
 971

972 Table 1. Natural variability of salinity and [Ca²⁺] in Kiel Fjord and Usedom.
973

Salinity (g kg ⁻¹)	Usedom	Kiel
Min.	3.44	10.50
1st Qu.	6.81	15.30
Median	7.19	17.10
Mean	7.14	17.15
3rd Qu.	7.74	18.90
Max.	9.33	24.70

[Ca ²⁺] (mM)	Usedom	Kiel
Min.	2.22	3.57
1st Qu.	2.67	4.97
Median	2.71	5.49
Mean	2.70	5.51
3rd Qu.	2.75	6.01
Max.	3.14	7.70

974
975
976
977
978
979
980
981
982
983
984
985
986
987
988
989
990
991
992
993
994
995
996
997
998
999
1000
1001
1002
1003
1004
1005
1006
1007
1008
1009
1010

1011 Table 2: Experimental conditions during larval experiments, N:1-10 determinations, $\Omega_{\text{Aragonite}}$
 1012 and $[\text{Ca}^{2+}][\text{HCO}_3^-]/[\text{H}^+]$ are calculated from measured $[\text{Ca}^{2+}]$, C_T and pH_{NBS} .

A) $[\text{Ca}^{2+}]$ manipulation experiments with *M. edulis*-like

$[\text{Ca}^{2+}]$ treatment	$[\text{Ca}^{2+}]$ (mmol/L)
<1 mM	0.86 ± 0.02
1.5 - 2 mM	1.56 ± 0.03
2.0 - 2.5 mM	2.19 ± 0.03
2.5 - 3 mM	2.82 ± 0.05
3.0 - 4.0 mM	3.62 ± 0.06
4.0 - 5.0 mM	4.42 ± 0.11
5.0 - 6.0 mM	5.74 ± 0.07
6.0 - 8.0 mM	6.83 ± 0.25
>8.0 mM	9.22 ± 0.10

B) $[\text{Ca}^{2+}]$ manipulation experiments with *M. trossulus*-like

$[\text{Ca}^{2+}]$ treatment	$[\text{Ca}^{2+}]$ (mmol/L)	$\Omega_{\text{Aragonite}}$	$[\text{Ca}^{2+}][\text{HCO}_3^-]/[\text{H}^+]$ [mmol][mol]/[μmol]
<1 mM	0.40 ± 0.02	0.16 ± 0.02	0.08 ± 0.01
1 mM	1.07 ± 0.04	0.43 ± 0.00	0.20 ± 0.01
1-1.5 mM	1.36 ± 0.00	0.51 ± 0.03	0.24 ± 0.01
1.5 - 2 mM	1.79 ± 0.03	0.62 ± 0.04	0.29 ± 0.02
2.5 - 3 mM	2.94 ± 0.03	0.98 ± 0.07	0.46 ± 0.03
3.0 - 4.0 mM	3.74 ± 0.04	1.23 ± 0.06	0.58 ± 0.03
>5.0 mM	5.78 ± 0.01	1.86 ± 0.11	0.88 ± 0.04

C) $[\text{Ca}^{2+}]$ and carbonate systems manipulation experiments with *M. edulis*-like

treatment	$[\text{Ca}^{2+}]$ (mmol/L)	$\Omega_{\text{Aragonite}}$	$[\text{Ca}^{2+}][\text{HCO}_3^-]/[\text{H}^+]$ [mmol][mol]/[μmol]
control + high C_T	0.93 ± 0.02	0.26 ± 0.07	0.18 ± 0.05
	1.55 ± 0.03	0.45 ± 0.09	0.31 ± 0.06
	2.25 ± 0.06	0.64 ± 0.15	0.44 ± 0.10
	2.99 ± 0.05	0.80 ± 0.22	0.55 ± 0.15
	3.69 ± 0.04	1.05 ± 0.23	0.73 ± 0.16
	5.45 ± 0.70	1.36 ± 0.04	0.94 ± 0.02
	8.69 ± 1.03	2.63	1.8
low C_T	0.92 ± 0.01	0.06 ± 0.01	0.04 ± 0.01
	1.59 ± 0.05	0.10 ± 0.03	0.07 ± 0.02
	2.25 ± 0.08	0.14 ± 0.03	0.10 ± 0.02
	2.78 ± 0.21	0.17 ± 0.02	0.12 ± 0.01
	3.37 ± 0.38	0.20 ± 0.01	0.14 ± 0.01
	5.88 ± 0.29	0.36 ± 0.06	0.25 ± 0.05

1013
 1014
 1015
 1016
 1017

1018 Table 3: Model parameters (a, b, c) describing PD I size as a function of experimental
 1019 seawater conditions for *Mytilus edulis*-like and *trossulus*-like: Shell length (μm) = $a + b * e^{c * [\text{parameter}]}$.
 1020

A) Seawater $[\text{Ca}^{2+}]$				
<i>M. edulis</i> -like	Estimate	std Error	t-value	p
a	112.7	1.8	63.4	<0.001
b	-100.7	7.6	-13.3	<0.001
c	-0.8	0.1	-9.3	<0.001
<i>M. trossulus</i> -like	Estimate	std Error	t-value	p
a	120.6	1.8	66	<0.001
b	-94.5	5.2	-18.1	<0.001
c	-1	0.1	-10.3	<0.001
B) Seawater $\Omega_{\text{Aragonite}}$				
<i>M. edulis</i> -like	Estimate	std Error	t-value	p
a	118.9	3.8	31.1	<0.001
b	-106.1	16.1	-6.6	<0.001
c	-3.1	0.6	-4.7	<0.001
<i>M. trossulus</i> -like	Estimate	std Error	t-value	p
a	121.6	2.3	53.5	<0.001
b	-100.8	6.4	-15.7	<0.001
c	-2.8	0.3	-9.0	<0.001
C) Seawater $[\text{Ca}^{2+}][\text{HCO}_3^-]/[\text{H}^+]$				
<i>M. edulis</i> -like	Estimate	std Error	t-value	p
a	125.9	5.0	25.3	<0.001
b	-73.5	4.3	-17.2	<0.001
c	-1.8	0.3	-5.9	<0.001
<i>M. trossulus</i> -like	Estimate	std Error	t-value	p
a	121.4	2.2	54.0	<0.001
b	-104.8	7.1	-14.9	<0.001
c	-6.0	0.7	-9.0	<0.001

1021
 1022
 1023
 1024
 1025
 1026
 1027
 1028
 1029
 1030
 1031
 1032
 1033
 1034
 1035
 1036
 1037
 1038
 1039
 1040
 1041

1042 Table 4: Results for linear models fitted on log transformed data of shell length and seawater
 1043 parameters, significant results in bold.

A) Response to $[Ca^{2+}]$

	Estimate	std Error	t-value	p
Intercept	4.17	0.07	59.2	<0.001
Ca²⁺	0.31	0.06	4.9	<0.001
population	0.12	0.04	2.8	<0.01
Ca ²⁺ :population	-0.01	0.04	-0.3	>0.05
F: 82.1		p: <0.001		R2: 0.77

B) Response to $\Omega_{Aragonite}$

	Estimate	std Error	t-value	p
Intercept	4.64	0.05	90.4	<0.001
$\Omega_{Aragonite}$	0.13	0.04	3.08	<0.01
population	0.04	0.03	1.23	>0.05
$\Omega_{Aragonite}$: population	0.1	0.03	2.86	<0.01
F: 116.4		p:<0.001		R2: 0.82

C) Response to $[Ca^{2+}][HCO_3^-]/[H^+]$ (CHH)

	Estimate	std Error	t-value	p
Intercept	4.69	0.08	60.1	<0.001
CHH	0.27	0.07	3.8	<0.001
population	0.13	0.05	2.5	<0.05
CHH: population	0.02	0.04	0.5	>0.05
F: 67.4		p: <0.001		R2: 0.78

1044